This information product has been peer reviewed and approved for publication as a preprint by the U.S. Geological Survey.

Cruise Summary

Gartman, A.[a*], Adamczyk, K.B. [a], Addison, J.A. [b], Bourque, J.R. [c], Caissie, B.E. [b], Caron, C.S. [c], Demopoulos, A.W. [c], Favela, J. [d], Ianiri, H.L. [a], Powers, D.C. [a], Prouty, N.G. [a], Rudebusch, J.A. [a], and Shapiro, I.M. [a]

a. U.S Geological Survey, Pacific Coastal and Marine Science Center, Santa Cruz, CA
b. U.S. Geological Survey, Geology, Minerals, Energy and Geophysics Science Center, Moffett Field, CA
c. U.S. Geological Survey, Wetland Aquatic Research Center, Gainesville, FL
d. National Oceanic and Atmospheric Administration Ocean Exploration Cooperative Institute, Narragansett, RI

*agartman@usgs.gov

Samoa Basin Abyssal Mapping: Box Coring Leg

2026-604-FA
OPR-T900-KR-26

M/V Ocean Guardian

April 11- May 1, 2026

Pago Pago, Territory of American Samoa to Pago Pago, Territory of American Samoa

Contents

Acknowledgements

We are grateful to the people of the Territory of American Samoa for their kind welcome and the opportunity to do this work in the Samoa Basin. We are grateful especially to Governor Pula, the staff of the Governor's office, Mike McDonald and the staff and leadership of the Port Authority for their welcome and facilitation of this work. Fa'afetai tele lava.

We are thankful to Captain Scott Dunaway and the officers and crew of the M/V Ocean Guardian for a safe and successful expedition. We thank Matt Hughes, Wyatt Buckson, Bradley Widman, Ricardo Zamora, Daniel Babin, Jonathan Raymond, Jack Hutchinson III, and Ethan Zehren for their work deploying and recovering the box core.

We'd also like to thank Michael Stephens at the National Oceanic and Atmospheric Administration, Erick Huchzermeyer at the Bureau of Ocean and Energy Management, and numerous colleagues at the USGS, BOEM and NOAA for their support, expertise and assistance in planning, coordinating, and conducting this expedition, as well as the Captain, crew, and scientific staff of the R/V Armada 86 05 for their efforts to share autonomous underwater vehicle

(AUV) data with us in time to inform our sampling strategy. This expedition was leg three of NOAA's American Samoa Abyssal Mapping effort, OPR-T900-KR-26, and data from legs one and two were critical to our effort.

We acknowledge support from the U.S. Geological Survey Mineral Resources Program, Coastal and Marine Hazards and Resources Program, the Outer Continental Shelf Program, and Ecosystems Land Change Science Program. We acknowledge Ocean Exploration Cooperative Institute support of Jaycee Favela. The USGS work on this effort was funded in part by the Bureau of Ocean Energy Management through Interagency Agreement M20PG00028 with the USGS. Any use of trade, firm, or product names is for descriptive purposes only and does not imply endorsement by the U.S. Government.

Shipboard Scientific Personnel

Person	Role	Science role
Katlin Adamczyk	Shift Lead	Sediment geochemistry, radon, Hg
Jason Addison	Project Scientist	Geochronology
Jill Bourque	Project Scientist	Biology
Beth Caissie	Project Scientist	Geochronology
Caroline Caron	Project Scientist	Biology
Jaycee Favela	Project Scientist	Rocks
Amy Gartman	Expedition Lead	Rocks
Dan Powers	Project Scientist	Coring and subcoring
Nancy Prouty	Project Scientist	Organic geochemistry
Maru Shapiro	Project Scientist	Sediment geochemistry

Abstract

This cruise report describes work from leg three of the NOAA American Samoa Abyssal Mapping effort, OPR-T900-KR-26. Leg one preceded this effort and collected ship-based acoustic data. Leg two collected autonomous underwater vehicle (AUV) data and began before, continued contemporaneously, and finished subsequently to leg three. The USGS field activity number assigned to this expedition is 2026-604-FA. The objective of this expedition was to collect representative box cores to inform prospectivity analyses through the region, and co-located interdisciplinary datasets as practical.

USGS personnel directed the sampling locations and took custody of the box cores once recovered shipboard. USGS personnel then photographed and described the cores, subsampled,

conducted analyses including wet weights and time sensitive measurements, and preserved subsamples and additional components for future work. Data releases co-released with this report are listed in the section "paired data releases." NOAA released data from all legs of this effort in near-real time. Details of the preceding legs, the data, and NOAA's project summary available from NOAA, (2026). This report is an expedition summary with preliminary datasets; remaining data releases and publications will be forthcoming.

Expedition Summary

USGS scientists led a box coring effort to the Samoa Basin, in order to characterize minerals and the surrounding abyssal sediments and fauna. Thirty-eight box cores were deployed between 4/13/2026 and 4/28/2026. Thirty-six box cores recovered some amount of sediment material, with 36 recovering sufficient material to determine nodule density, and 35 recovering sufficient material for subcores to be collected. Of these, 35 were deployed in the "high" priority area bordered in the west by Rose Atoll National Monument and seamount chain, and in the east, north, and south by the boundaries of the U.S. EEZ. One box core was deployed in the "medium" priority area, north of Rose Atoll National Monument (Figure 1).

The selection of twenty-nine of the box core locations were guided by AUV data, which was collected before and after the box coring expedition. The remaining nine cores were deployed in regions that did not yet have AUV data (BX10, 12, 14, 15, 16, 21, 22, 36 and 38), and were informed by ship based bathymetry and principles of sample distribution. Sample distribution aimed to collect from all regions at the highest end of nodule density for the dataset, as well as representative samples in the same regions without nodules and with lower densities. Box core locations were chosen to be within the center of collected of AUV datasets (NOAA, 2026), however due to positioning uncertainty it is not clear whether box core landed within AUV's

Cathex imagery data (NOAA, 2026), which has a footprint of 180 m N-S and 90 m E-W.

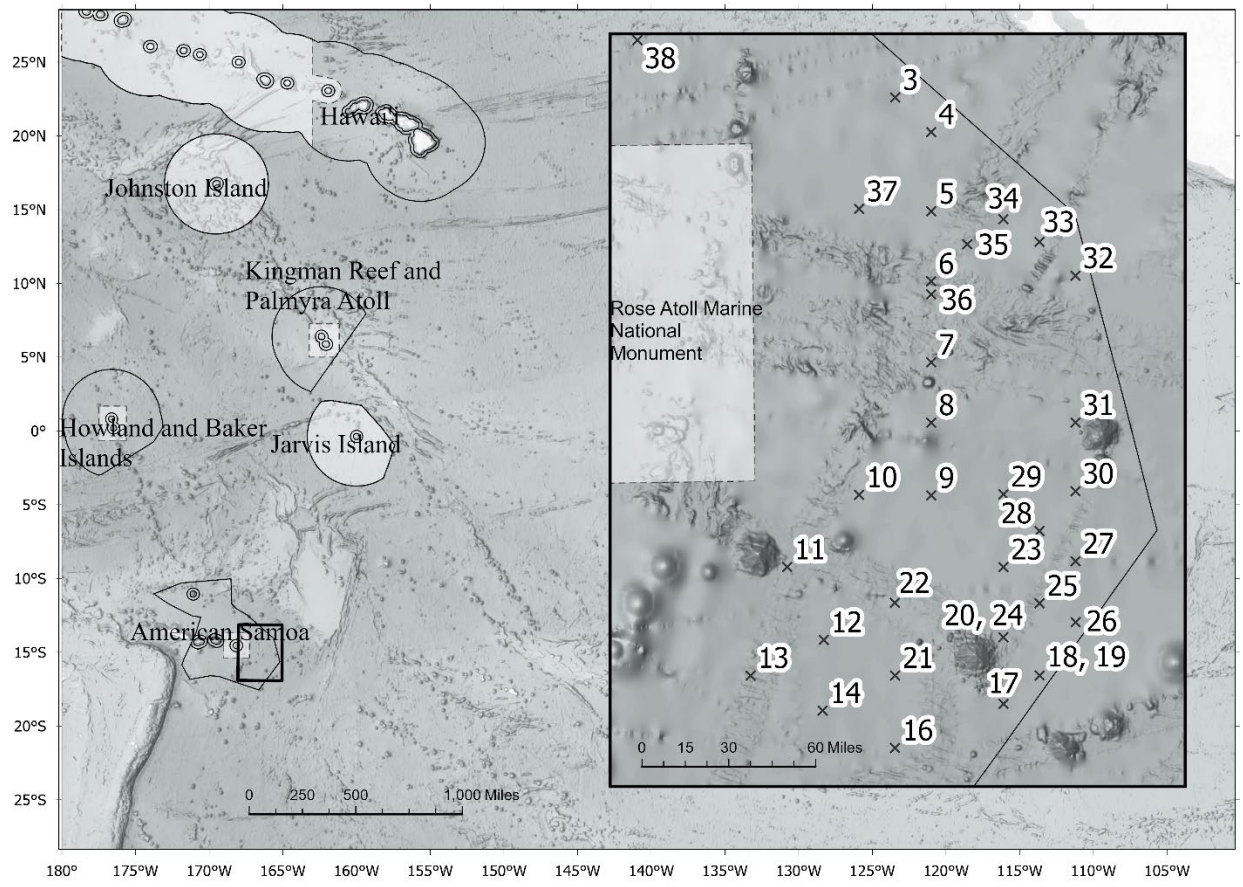

Figure 1. Overview map of the region of interest, and the numbered box core locations, inset map. Map data sources: ESRI, TomTom, Garmin, FAO, NOAA, USGS © OpenStreetMap contributors, and the GIS User Community, General Bathymetric Chart of the Oceans (GEBCO); NOAA National Centers for Environmental Information (NCEI).

Sample positioning

Sample positioning was derived from ultrashort baseline (USBL) acoustic position where available, and from the ship's position where USBL data were unavailable. A 7000-m rated USBL (Kongsberg MiniS 37-40V Ti; Kongsberg Group, Kongsberg, Norway) was attached to the box core wire for all dives. Box cores BX6-16, BX18- 24, and BX26-38 returned some USBL data. Of those, all except BX38 lost contact with the USBL before hitting the bottom. For box cores with functioning USBL data, the location given is the location at the deepest recorded depth of the box core when either the upcast or downcast returned data (BX06, BX28) or the midpoint between the deepest depth recorded on the downcast and the deepest depth recorded on the upcast when both the upcast and downcast returned data (BX7-16, BX18-24, BX26-27, BX29-37). For BX38, the USBL position when the box core hit bottom is reported. For box

cores without USBL data, the position of the ship when the box core was deployed is reported (BX03-BX05, BX17, BX25). The distance between the ship's GPS and the box core's seafloor location determined by the midpoint of the USBL data is generally less than 50 m. Depth is derived by adding 2 m from the conductivity, temperature, and depth (CTD) data. This information, along with the ship's coordinates for all samples is given in Adamczyk and others, (2026).

Table 1. The date, time, and location for all deployed box cores. The superscript letter "s" indicates that the location is the ship's position and that USBL data were not available for that cast.

Date on bottom (UTC)	Time on bottom (UTC)	Core #	Near node	Latitude	Longitude	Depth (m)
4/13/2026	22:51	BX01	5K	-13.83505 ^{s}	-166.91699 ^{s}	5440
4/14/2026	9:44	BX02	7L	-13.46979 ^{s}	-166.5427 ^{s}	5643
4/14/2026	19:00	BX03	7L	-13.46984 ^{s}	-166.54275 ^{s}	5644
4/15/2026	4:40	BX04	8K	-13.64489 ^{s}	-166.35907 ^{s}	5426
4/15/2026	14:41	BX05	8J	-14.04159 ^{s}	-166.36119 ^{s}	5494
4/16/2026	0:16	BX06	8I	-14.393338	-166.364138	5668
4/16/2026	9:54	BX07	8H	-14.799256	-166.365759	5563
4/16/2026	19:14	BX08	8G	-15.102337	-166.367613	5537
4/17/2026	4:46	BX09	8F	-15.467845	-166.36995	5476
4/17/2026	14:22	BX10	6F	-15.461795	-166.743806	5492
4/18/2026	1:06	BX11	4E	-15.820406	-167.119892	5787
4/18/2026	11:04	BX12	5DE	-16.188038	-166.933108	5665
4/18/2026	20:58	BX13	3C	-16.363028	-167.315438	5655
4/19/2026	6:33	BX14	5CD	-16.542541	-166.942896	5586
4/19/2026	17:41	BX15	5B	-17.035401	-166.972696	5587
4/20/2026	4:21	BX16	7C	-16.732792	-166.568031	5579
4/20/2026	15:45	BX17	10A	-16.51513 ^{s}	-166.00112 ^{s}	5656
4/21/2026	0:34	BX18	11A	-16.37385	-165.812611	5670
4/21/2026	7:21	BX19	11A	-16.37387	-165.812872	5667
4/21/2026	15:37	BX20	10B	-16.181011	-165.99996	5420
4/22/2026	2:31	BX21	7D	-16.369757	-166.564505	5699
4/22/2026	12:07	BX22	7E	-16.004886	-166.562444	5578
4/22/2026	23:13	BX23	10C	-15.829178	-165.997863	5598
4/23/2026	8:20	BX24	10B	-16.181125	-166.000636	5419
4/23/2026	17:14	BX25	11B	-16.01167 ^{s}	-165.81103 ^{s}	5644
4/24/2026	1:50	BX26	12A	-16.106676	-165.624108	5724
4/24/2026	12:14	BX27	12B	-15.801111	-165.623754	5578
4/24/2026	20:37	BX28	11C	-15.648456	-165.809922	5537
4/25/2026	5:40	BX29	10D	-15.463835	-165.996259	5498
4/25/2026	14:57	BX30	12C	-15.449997	-165.622993	5599
4/26/2026	1:23	BX31	12D	-15.105277	-165.621656	5613

4/26/2026	13:13	BX32	12F	-14.368471	-165.620218	5501
4/26/2026	21:18	BX33	11G	-14.197736	-165.804495	5417
4/27/2026	5:36	BX34	10H	-14.083602	-165.990383	5511
4/27/2026	13:33	BX35	9H	-14.20833	-166.17707	5478
4/27/2026	22:29	BX36	8Isouth	-14.458745	-166.363834	5412
4/28/2026	8:47	BX37	6J	-14.027291	-166.731756	5534
4/28/2026	1:06	BX38	16A	-13.170653	-167.861665	5184

Rocks and minerals

Summary

Ferromanganese minerals were sampled within the Samoa Basin. Nodule morphologies included spheroidal, ellipsoidal, polynucleate, and pebble morphologies; occasional stick nodules were also collected. Not all collected ferromanganese minerals were nodules; thinly coated volcanic material, cobbles, coated shark teeth, and ferromanganese plates were also collected. Nodule surficial texture was most commonly granular but botryoidal textures were also observed.

Throughout the 38 box cores collected, nodule morphology, density, and total mass varied and informed the sampling approach.

Of the 38 box cores collected, 26 box cores have sample material that was collected for geochemical analysis. “Material” includes nodules and the contents from BX13 which was described shipboard as coated scoria or volcanic rock possibly coated in ferromanganese. All other box cores not sampled for geochemistry either did not have nodules or did not have sufficient material for analysis.

Nodule abundances ranged from zero to 21 kg/m^2 (Figure 2, 3). For most boxes, the surface nodules comprised all of the nodules collected; however, there were four locations, including the densest site, in which buried nodules made a meaningful fraction of the total. Surface nodule abundance ranged from zero to 18.5 kg/m^2. For comparison, Figure 4-11 in Tay and others, (2023), indicates the four quartiles for nodules from the adjacent Penrhyn Basin are: Q_1 3.18, Q_2 13.44, Q_3 22.23 kg/m^2, and Q_4 62.91 kg/m^2.

Two duplicate boxes were collected, where the box core was dropped in nominally the same location ($\pm$ 50 m, within error of the USBL). The duplicates are BX18 and BX19 (duplicate 1) and BX20 and BX24 (duplicate 2, Adamczyk et al., 2026). The variability of nodule abundances for the duplicates was approximately 15%.

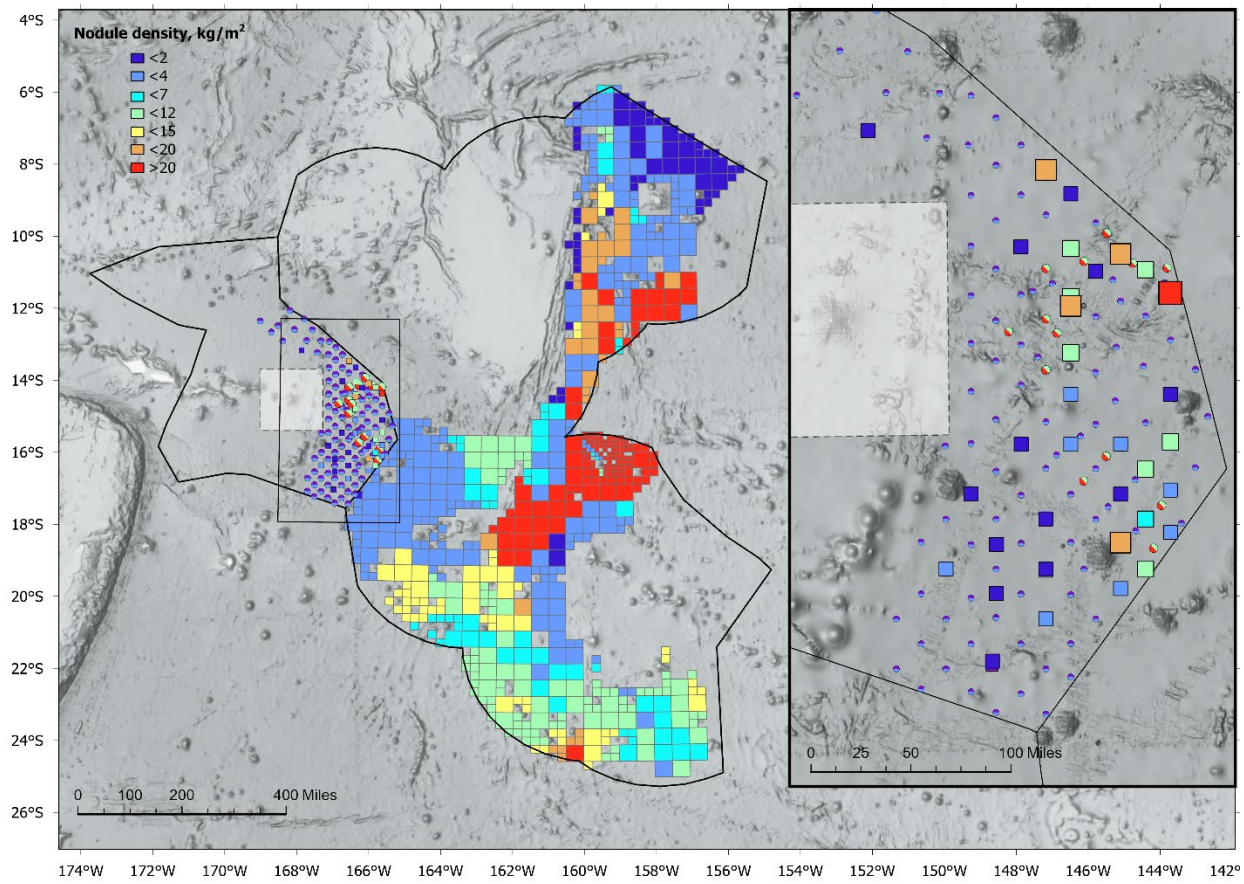
Nodule density, kg/m²
<2
<4
<7
<12
<15
<20
>20
0 100 200 400 Miles
0 25 50 100 Miles
4°S
6°S
8°S
10°S
12°S
14°S
16°S
18°S
20°S
22°S
24°S
26°S
174°W
172°W
170°W
168°W
166°W
164°W
162°W
160°W
158°W
156°W
154°W
152°W
150°W
148°W
146°W
144°W
142°

Figure 2. Map of nodule abundances measured in box cores in the Samoa Basin collected in this expedition displayed next to modeled abundances from the Cook Islands Seabed Mineral Authority, https://www.sbma.gov.ck/maps. The U.S. Exclusive Economic Zone around American Samoa (western polygon) and the Cook Islands Exclusive Economic Zones (eastern polygon) abut, and are both outlined in black.

The inset shows density of polymetallic nodules (kg/m^2) measured from box cores collected on this expedition (square symbols) along with coarsely estimated abundances from AUV imagery, small circles. AUV data were assigned either colors consistent with the first two quartiles, or the third quartile and maximum. Quartile information is given in figure 2, below. The white box surrounded by a dashed line in the center of the U.S. Exclusive Economic Zone is the Rose Atoll Marine National Monument.

For the data underlying the SBMA model, refer to figure 4-11 in Tay and others, (2023).

Map data sources: ESRI, TomTom, Garmin, FAO, NOAA, USGS © OpenStreetMap contributors, and the GIS User Community, General Bathymetric Chart of the Oceans (GEBCO); NOAA National Centers for Environmental Information (NCEI)

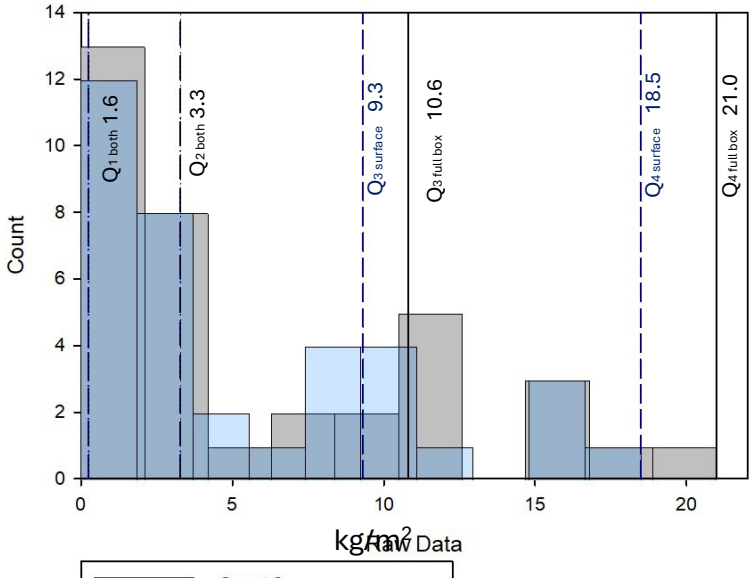

Figure 3. Histogram of nodule abundance with quartiles. Surface abundances are given in blue, and total box abundances, which include buried nodules, are given in grey. Q_1-Q_2 values are the same for both surface and buried nodules; Q_3 and Q_4 values are different, and both values are listed.

Geochemical results of the ferromanganese rocks, and analytical details are contained in Adamczyk and others, (2026). Average data for the nodule samples are presented in Table 2; ferromanganese coated sediments and volcanic rocks are excluded from the average.

Geochemically, nodules from the Samoa Basin are similar to those from the adjacent Cook Islands' EEZ, specifically those of the western and south Penrhyn Basin (Tay and others, 2023). Samples are higher in iron and cobalt, and lower in copper and nickel, than average nodules from the Clarion Clipperton Zone to the northwest.

Table 2. Chemical compositions of nodules from the Territory of American Samoa compared to nodules from the Cook Islands (CI) and the Clarion Clipperton Zone (CCZ). Territory of American Samoa data are the average of surface nodule samples contained in Adamczyk and others, (2026). CI and CCZ data are from Mizell and others, (2022).

Element (symbol)	Territory of American Samoa	Cook Islands	Clarion Clipperton Zone
Fe (wt %)	16.6	16.2	5.99
Mn	16.2	16.9	28.4
Si	9.00	7.03	6.10
Al	3.97	3.42	2.32
Ca	2.04	1.99	1.68
Mg	1.39	1.42	1.94
Na	1.51	1.76	2.16
K	0.93	0.90	0.98
Ti	1.29	1.28	0.27
P	0.37	0.34	0.16
		(ppm)	
Ag (ppm)	0.07	0.23	0.30
As	162	150	82
Ba	1156	1160	3933
Be	4.8	3.9	2.2
Bi	11	11	8.8
Cd	4.4	4.7	16
Cl	10,972	-	-
Co	3,605	3,751	1,918
Cr	37	59	12.4
Cs	0.53	0.38	1.3
Cu	1,961	2,309	10,794
Ga	16	-	-
Ge	1	-	0.70
Hf	12	13	4.6
		(ppb)	
Hg (ppb)	8.5	36	18.0
		(ppm)	
In (ppm)	0.73	0.78	0.27
Li	42	51	132

Element (symbol)	Territory of American Samoa	Cook Islands	Clarion Clipperton Zone
Mo (ppm)	256	295	612
Nb	90	91	19
Ni	3,230	3,767	12,785
Pb	861	976	358
Rb	16	15	21
S	1,623	1,829	1,572
Sb	32	36	65
Sc	14	12	10
Se	8.9	0.80	0.72
Sn	4.4	7.8	5.3
Sr	976	935	691
Ta	2.7	2.2	0.27
Te	22	24	3.6
Th	35	36	199
Tl	111	146	14
U	9.2	9.5	3.9
V	521	504	591
W	52	59	63
Zn	479	492	1,509
Zr	572	555	287
La	173	173	106
Ce	1,058	991	283
Pr	43	41	31
Nd	173	160	126
Sm	39	35	31
Eu	9.4	8.5	7.6
Gd	40	36	30.4
Tb	6.5	6.1	4.6
Dy	39	35	27
Y	148	141	83
Ho	7.6	7.2	4.9
Er	22.0	19.1	13.4
Tm	3.1	3.0	1.9
Yb	21.0	19.8	12.9
Lu	3.4	3.0	1.9
Sum REY	1,786	1,678	764

Sampling, subsampling, and paired analyses

After removing topwater and photographing the core surface, nodules were removed, weighed, and photographed. They were then either rinsed in freshwater, dried, and packed for compositional analysis, stored in seawater for additional mineralogic work, or frozen for future analysis. In addition to compositional analysis and mineralogy, nodules will be analyzed for microbiology, total organic carbon, radon, and mercury speciation. Details of those analyses are given in their respective sections.

Nodule samples from 18 box cores were processed and stored in jars in seawater for future analyses. Analyses are to be carried out at the U.S. Geological Survey office in Santa Cruz, CA as part of the USGS Global Seabed Minerals and Resources Project (https://www.usgs.gov/centers/pcmsc/science/global-seabed-mineral-resources).

Buried nodules

Four sites (BX03, BX32, BX33, and BX36) had quantifiable concentrations of buried ferromanganese minerals. In three of these sites the buried ferromanganese was nodules. In one site the buried ferromanganese was a mixture of nodules and coated cobbles. Care was taken to divide rocks that could have been pushed down by the spade and occurred along the sides or bottom of the box, from those rocks that appeared to have been actually buried, and which were located more centrally in the box. Nodules that seem to have been pushed down by the spade were included in the surface totals, rather than the buried totals. All nodules found in the box, regardless of location, were included in the "full box" totals. We note that the box density is presented as a mass per square meter measurement, and for buried nodules a mass per cubic meter measurement would be a more accurate; however the data are presented in this manner for consistency with convention, as most previous work does not treat buried nodules separately.

Sediment Biology, Geochronology, and Geochemistry

Summary

Following the removal of rock and mineral samples (when present) the box core was subsampled for biological, geochronological, and geochemical analyses. Two sterilized 60-mL syringes and one 2-cm deep plastic fence were inserted into the sediment surface to collect samples for metagenomic and eDNA analysis. Following the collection of these samples, a mechanical subcoring device fit with a piston was used to collect 9-cm diameter push cores while minimizing sediment compaction. Three push cores had pre-drilled holes spaced at 1-cm intervals for microprofiling (PC01), porewater extraction (PC02), and mercury sampling (PC04). Three push cores without pre-drilled holes were collected for organic carbon (PC03), geochronology (PC05), and geochemistry and mineralogy (PC06) subsampling. Four 6.35-cm diameter push cores were hand-pushed into the upper 10-cm of sediment to be subsampled and sieved for infauna. One or two 4-cm fences were inserted into the surface sediment (at 10 box core locations) for radon flux measurements. The upper 2-cm of sediment was scraped from around the placed push cores, prior to their removal, to be sieved for infauna. Push cores were removed from the box core, capped, and transferred to a cold laboratory van (set to 7 °C) within 1-2 hours of box core recovery. Each push core was photographed and described before subsampling and analysis (outlined below).

Biological Summary

Biological samples were collected from the box cores to assess sediment community composition across the range of nodule density habitats. Across the cruise, topwater, surface scrapes (0-2 cm), and subsamples for future whole community eDNA analysis were collected from 35 box cores, and four replicate push cores were collected on 34 box cores. Topwater, surface sediments, and vertical fractions (0-2 cm, 2-5 cm, and 5-10 cm) from three push cores were sieved through a 300-µm sieve and sorted for visible animals under a dissecting microscope. Additionally, nodules were inspected for attached epifauna that were collected when present. All animals were documented with photographs and preserved in 95% ethanol.

Preliminary analysis of animals collected totaled 262 individuals (Table 3), including 133 sediment macrofauna (>300µm), 95 large sediment meiofauna, 20 epifauna, and 14 benthopelagic individuals (Table 3). Most sediment macrofauna taxa collected were crustaceans (51 %), dominated by the peracarid groups Isopoda (at least 7 families) and Tanaidacea. Polychaeta comprised 26% of the taxa collected, including at least 5 families currently identified. The remaining individuals were comprised of molluscs (12 %), Ophiuroidea (10 %), and two unknown individuals (1 %; Figure 4, 5). Large sediment meiofauna were collected, with taxa dominated by copepods, followed by nematodes and ostracods. Very few nodules housed epifauna, with taxa found comprised primarily of sponges (Porifera); however, a few individual Bryozoa, Tunicata, Brachipoda, and a barnacle were also collected. Although not targeted, a few benthic-associated (benthopelagic) organisms were collected from the topwater samples, including chaetognaths (arrow worms), shrimp, and a planktonic crustacean. Further taxonomic identifications will be performed at the laboratory to determine biodiversity estimates.

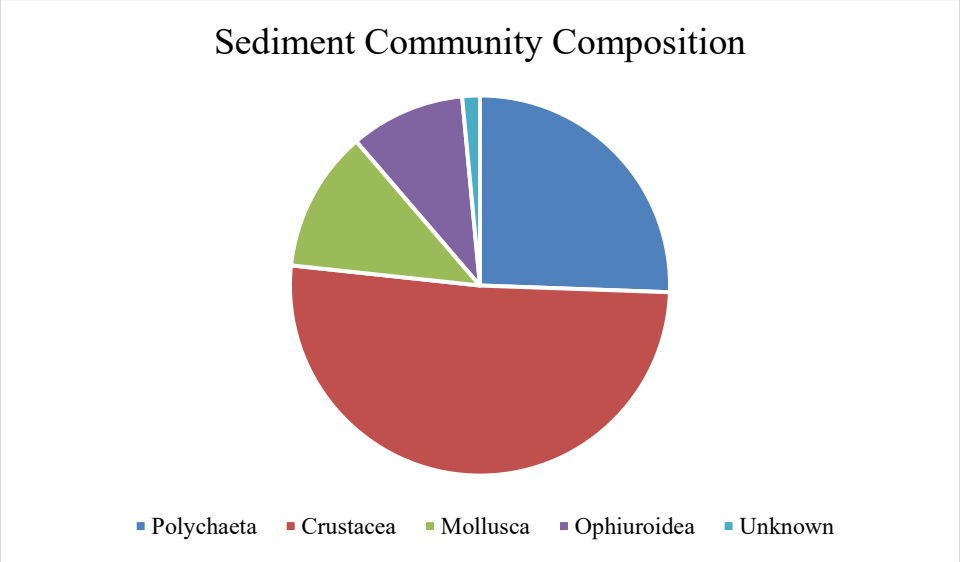

Figure 4. Proportional sediment community composition of macrofauna collected.

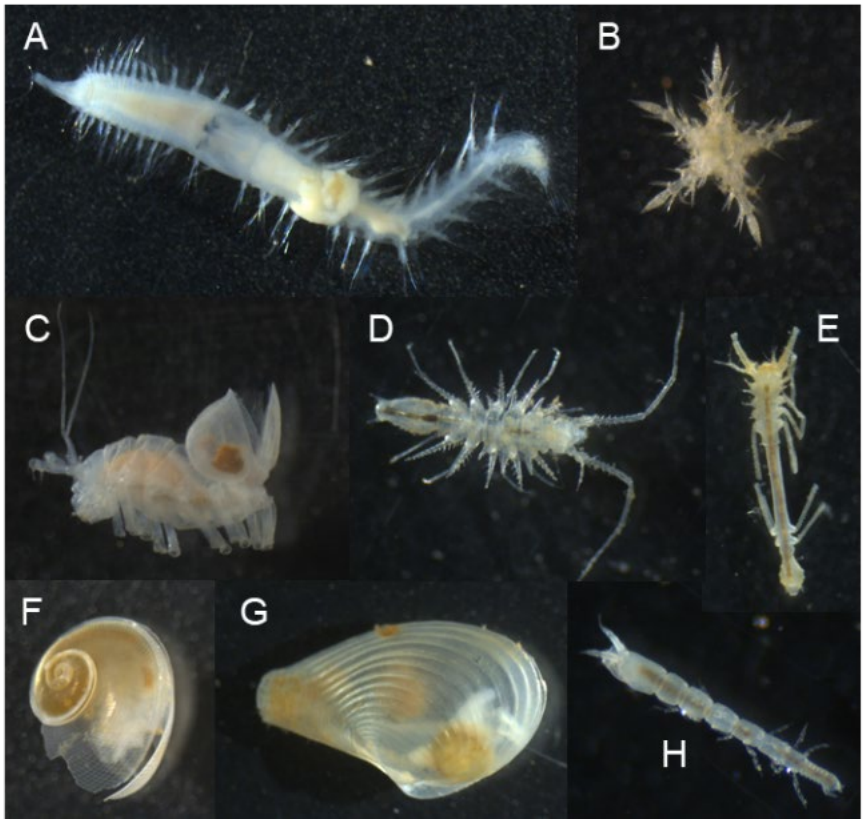

Figure 5. Macrofauna collected from box cores on 2026-604-FA. A) Glyceridae (Polychaeta); B) Ophiuroidea; C) Munnopsidae (Isopoda); D) Mesosignidae (Isopoda); E) Ischnomesidae (Isopoda); F) Scissurellidae (Gastropoda); G) Cuspidariidae (Bivalvia); H) Agathotanaidae (Tanaidacea). Credits: U.S. Geological Survey, photos by J. Bourque and C. Caron.

Table 3. Numbers of individual taxa collected from box cores on 2026-604-FA.

Taxa Group	N
Sediment Macrofauna	133
Polychaeta	34
Cirratulidae	3
Glyceridae	6
Nephtyidae	3
Paraonidae	3
Phyllodocidae	2
Unknown	17
Crustacea	68
Amphipoda	6
Cumacea	1
Isopoda	30
Tanaidacea	31
Mollusca	16
Gastropoda	3

Bivalvia	13
Ophiuroidea	13
Unknown	2
Sediment Meiofauna	95
Crustacea	76
Ostracoda	10
Copepoda	66
Nematoda	19
Benthopelagic	14
Chaetognatha	8
Shrimp	5
Crustacea	1
Epifauna	20
Brachiopoda	1
Bryozoa	2
Barnacle	1
Porifera	15
Tunicata	1
Total Animals	262

Microbiology

Duplicate sediment subsamples from each core were collected from the upper 10 cm of each core for 16S, 18S, ITS, rRNA sequencing to be conducted by Dr. Roxanne Beinart at the University of Rhode Island (URI).

Additional subsamples for microbiology were collected in coordination with the organic geochemistry core. The top surface of PC03 was subsampled for microbiology using a pre-cleaned spatula with RNase-away™ (Thermo Scientific™, Waltham, MA) and preserved with 9-ml DNA/RNA-Shield in 15-ml conical vials and kept frozen in -80°C freezer.

In collaboration with Dr. Roxanne Beinart, metagenomic sequencing data from the upper 10 cm of each box core station will be queried for mercury cycling genes - hgcAB which encodes proteins that methylate mercury, and merB which encodes a protein that breaks down methylmercury. Additionally, downcore metagenomic samples were collected from 5 subcores from boxes that had zero (n = 2), sparse (n = 1), or dense (n = 2) nodule coverage.

Nodule biofilm surface swabs were collected from 23 box cores and microbiology samples were collected from 25 box cores. Sample material mainly included nodules and occasionally volcanic rock material. Biofilm surface swabs were taken from the exterior of nodules that were subsequently measured for weight/dimensions and then transferred to be processed for geochemistry. For box cores that had distinct nodule morphologies and/or abundant sample

material, several nodule pieces were selected. Biofilm surface swab and microbiology analyses are to be carried out by Dr. Beinart at URI.

Geochronology

Samples Collected and Methodology

The geochronology team collected a variety of samples. Quick reconnaissance was done while on site to determine whether full cores should be taken for further analysis on shore. First, 20 cubic centimeter (cm^3) scoops were collected from the surface sediments from each box (n = 35). In two cores (BX01 and BX02), a smaller amount was scraped off the inside of the boxes when they did not trigger correctly and came up empty. In addition, 20 cm^3 scoops were also collected from the base of the box core on three occasions (BX11, BX34, and BX37). The scrapes from the base were collected based on suspicion of a layer of tephra at the base of the box core, however only BX11 had substantial tephra shards at its base.

The 20 cm^3 scoops and side scrapes were immediately made into smear slides for transmitted light microscopy and the remaining sediment sieved at 63 µm. This coarse fraction was examined under a stereo microscope at 6-50 X magnification. The microscope slide was then examined under a transmitted light microscope at 200-630 X magnification. In both cases, the biogenic components, in particular fish teeth, radiolarians, and diatoms were of interest. Slides and sieved fractions were qualitatively assessed using a 5-point scale where dominant (D) was > 50% of the components, abundant (A) was 25-50 %, common (C) was 5-25 %, rare (R) was 1-5 %, and trace (Tr) was <1 %.

Full cores (geochronology cores, designated as PC-05) were collected at 21 sites (Table 4, Figure 6). At one additional site (BX08), PC01 was sliced and bagged because of the large number of fish teeth discovered in the sieved fraction after the box had been washed out. Cores were extruded in 1 cm slices from 0-20 cm and in 2 cm slices below. Cores ranged from 30.5-43 cm in length.

Samples for shipboard X-ray fluorescence (XRF) analysis were collected from the upper ~2 cm of each boxcore (n = 36) and placed in clean petri dishes, which were then oven-dried at 40° C for 2 days. Each dry sample was ground to a homogenous fine powder in a ceramic mortar and pestle, and then loaded into a loose-powder sample cup equipped with a 4 µm- thick polypropylene X-ray transparent thin film with a polyfill backing to minimize porosity.

Each sample was analyzed in triplicate on a Bruker (Billerica, Massachusetts) Tracer 5i portable XRF in lab bench mode, where the loose-powder sample cup was placed directly on the XRF measurement window underneath a shielded chamber. Samples were run in batches of 5 or more, with both an instrument monitor (pure SiO_2) and manufacturer standard (Bruker mudrock tile) run in triplicate both before and after the samples. In addition, two Certified Reference Materials

(CRMs) were analyzed as part of each analytical batch (marine sediment standards MAG-1 and MESS-4) to assess instrument accuracy.

Table 4. List of sites visited with length of core extruded and collected by the geochronology group. NA, not applicable

Box	Site	Length of core extruded (cm)
BX01	5K	NA
BX02	7L	NA
BX03	7L	38
BX04	8K	37
BX05	8J	36
BX06	8I	35
BX07	8H	35
BX08	8G	41
BX09	8F	0
BX10	6F	39
BX11	4E	36
BX12	5D/5E	0
BX13	3C	40
BX14	5C/5D	0
BX15	5B	31
BX16	7C	0
BX17	10A	36.5
BX18	11A	33
BX19	11A	0
BX20	10B	0
BX21	7D	36.5
BX22	7E	0
BX23	10C	34
BX24	10B	35
BX25	11B	0
BX26	12A	0
BX27	12B	36
BX28	11C	0
BX29	10D	37
BX30	12C	37
BX31	12D	35
BX32	12F	0
BX33	11G	30.5

BX34	10H	0
BX35	9H	0
BX36	8I	0
BX37	6J	39
BX38	16A	43

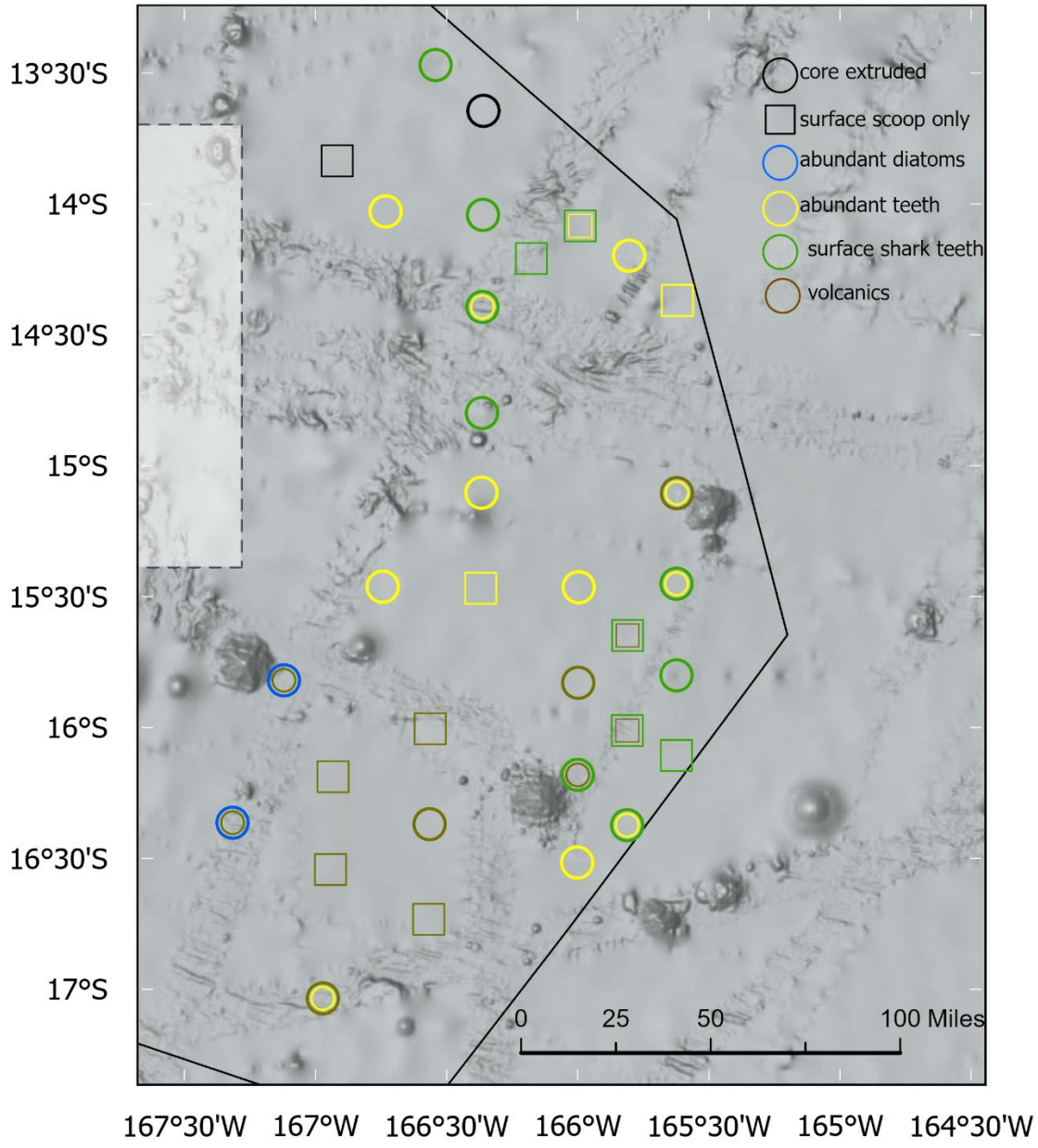

Figure 6. Sample map for geochronology team. Refer to legend on right for color coding and symbology. Map data sources: ESRI, TomTom, Garmin, FAO, NOAA, USGS © OpenStreetMap contributors, and the GIS User Community, General Bathymetric Chart of the Oceans (GEBCO); NOAA National Centers for

Environmental Information (NCEI)BX38, which is outside of the boundaries of this map, was classified as abundant diatoms and abundant teeth.

Summary of Results

Smear Slides

In general, smear slides were made up of 95-100% minerogenic grains with far fewer biogenic grains. The minerogenic component was subrounded to subangular and dominated by diffuse clay with opaque minerals (such as Fe_2O_3 or MnO_2) common. In some cases, clays clustered into mm-scale oval shaped clods with clusters of opaque minerals in the center. Other minerals included silt to sand sized quartz, goethite, zeolites, feldspar, and ferromagnesian minerals. In some cases, tephra was present, in particular in the southern half of the study area. In fact, BX11 had a thick layer of tephra at its base. This was identified by the unusual dry, crumbly texture in the box core and the dominance of tephra shards in the smear slide. The biogenic component included sponge spicules, radiolarians, diatoms, and silicoflagellates in trace to rare abundances. The final site (BX38) was significantly more biogenic than other sites with abundant radiolarians and rare diatoms present. Most samples had a clay texture with the exception of the rock scrape (Figure 7) and were moderately well to well sorted. Eleven sites had magnetic grains (BX04, 06, 08, 09,13,17, 23, 28, 29, 37, and 38).

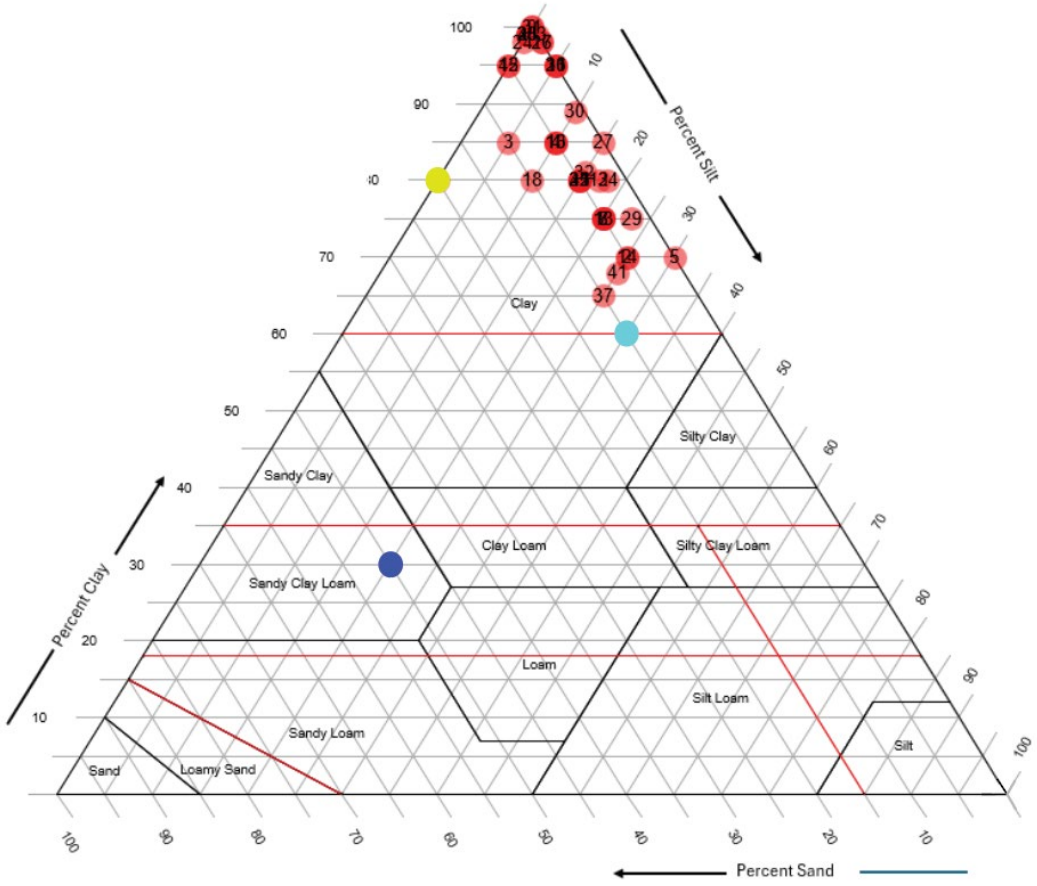

Figure 7. Triangular texture plot showing the relative proportions of clay, silt, and sand based on visual smear slide observations. Most samples from the study area are red circles. The yellow circle is the test site, the light blue circle is the last site (BX38), and the dark blue circle is the scrape from a welded tuff.

Coarse (>63 µm) Fraction

The coarse fraction was significantly more biogenic than the smear slides. The dominant components of the coarse fraction included fish teeth, radiolarians, sponge spicules and pieces, tephra shards, agglutinated foraminifera, and micronodules. Fish teeth were not counted in every sample, but for samples in which they occurred, counts ranged from 5 to 27 teeth per 20 cm^3 sample.

Surface sediment X-Ray Fluorometry (XRF) Geochemistry

Comparisons between the recovered boxcore surface sediment compositions and the paired certified reference material (CRM) standards (both of which are continental shelf-derived siliciclastic sediments low in carbonate concentrations) show that the BX sediments are rich in metals, particularly Fe, Mn, Ni, and Cu; the elements Ca, P, Sr, and As show also some enrichment. The BX sediments also appear to be depleted in other elements relative to the CRM standards, including Al, Si, K, Rb, and Ba.

The elemental ratio calculations of Bostrom (1973) or Strakhov (1976) allow us to assess if these sediments would be classified as metalliferous [as recounted in Gurvich (2006)]. The mean concentrations of Fe (7.48 wt%), Mn (1.016 wt%), Al (6.94 wt%), and Ti (0.791 wt%) from all of the BX sites suggest that these sediments would not meet their standards for categorization as metalliferous. Furthermore, the less stringent classification of Lisitzin and others (1976) that sediments merely need to contain >10 wt% abiotic Fe and also be depleted in Al and Ti to be metalliferous is also not met, although comparisons between the BX sediments and both MAG-1 and MESS-4 show that these sediments are indeed enriched in Fe and Mn, and depleted in Al.

Of particular interest for ongoing paleoceanographic studies of halide occurrence in marine sediment deposits, the element Br has a mean and 1s standard deviation across all sites of 272 ± 17 ppm, which surprisingly places the BX surface samples in the same range as typical high-productivity continental shelf settings along the US West Coast. This finding is puzzling as other indicators of productivity (e.g., phytoplankton occurrence in smear slides) show these deep-sea abyssal plain deposits to be exceedingly low productivity.

Applying a preliminary multivariate hierarchical cluster analysis to the BX dataset (BX03 to BX36) shows some geochemical differences between the sites (Figure 8). When the resulting three dominant clusters are plotted on the sampling map (Figure 9), we find that there are coherent geochemical “provinces”, with one distinct province in the northern end of the study area, as well as two provinces in the south.

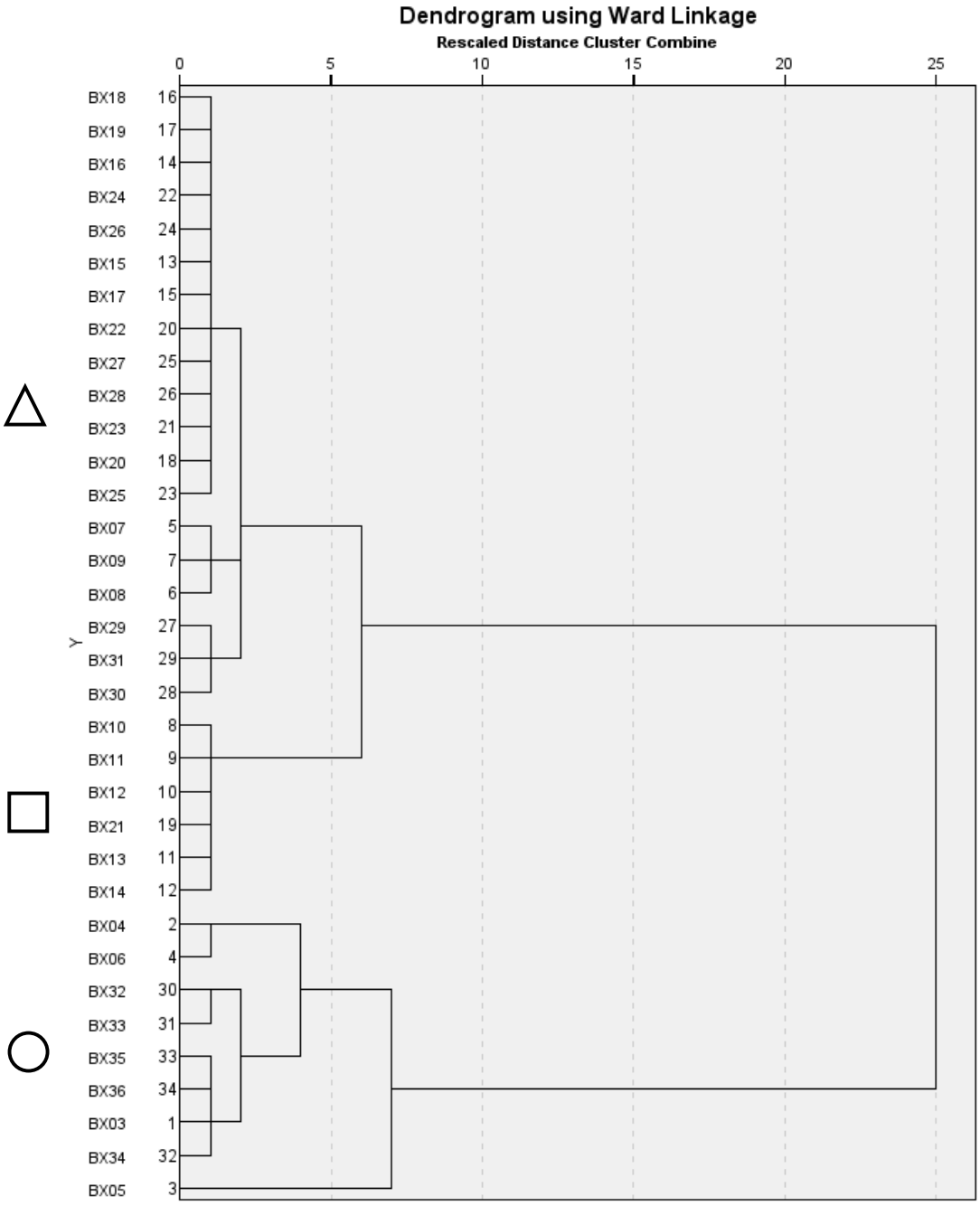

Figure 8. Multivariate hierarchical cluster analysis of surface sediment XRF results using 24 elements (excluding Na and Cl, as these are mostly associated with the presence of salt water in the samples). Analysis was performed in SPSS v.31. Input data were standardized to Z-scores and the clustering method was performed according to Ward's method using squared Euclidean distance measures (Shari and others, 1999).

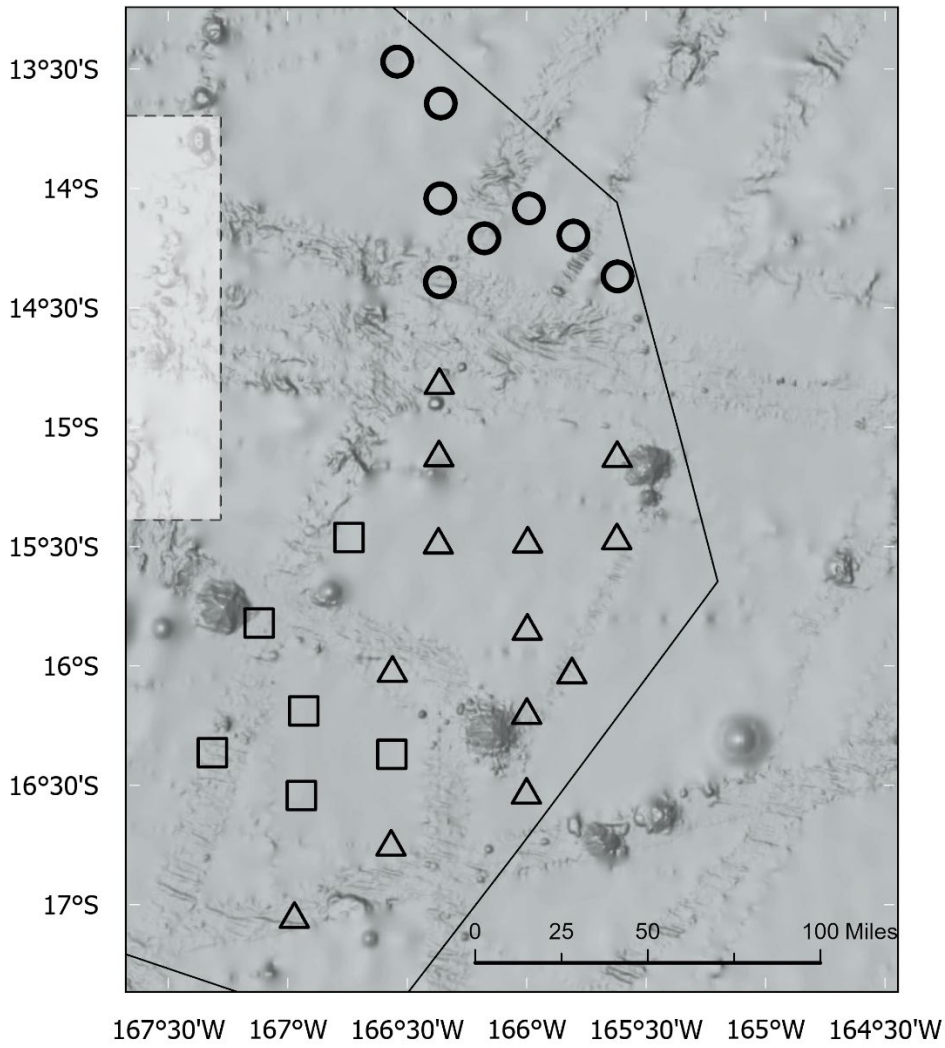

Figure 9. Map depicting clusters of XRF elemental data. Data for this Figure are contained in Addison and others, 2026. Map data sources: ESRI, TomTom, Garmin, FAO, NOAA, USGS © OpenStreetMap contributors, and the GIS User Community, General Bathymetric Chart of the Oceans (GEBCO); NOAA National Centers for Environmental Information (NCEI)

Planned Analyses

Radiolarian and possibly diatom biostratigraphy will be conducted on five sites in conjunction with a preliminary analysis of the $^{86}Sr/^{87}Sr$ composition of fish teeth at the same sites. We expect this work to provide us with several independent age models for the push cores. In addition, we will conduct a hyperspectral analysis and point-source magnetic susceptibility on archive halves of PC06 mineralogy cores stored at the U.S. Geological Survey in Santa Cruz, CA.

Sediment geochemistry summary

Shipboard work

There are four separate workflows associated with sediment geochemistry. One subcore from each box (PC06) was preserved for further analysis at the USGS Core Laboratory in Santa Cruz, CA (n = 35). Two subcores from each box were associated with porewater analyses (PC01 and PC02, described below). One subcore from each box (PC04) was subsampled for mercury and methylmercury analyses.

Pore water analysis

Pore water analysis comprised both porewater extraction and shipboard microprofiling. Microprofiles were measured in one subcore (PC01) from each box core (n = 35 cores; BX03-BX38, excluding BX16). Shipboard microprofiling was completed using Unisense Scientific (Aarhus, Denmark) oxygen (OX-100, OX-200, OX-NP), redox (RD-100, RD-200), and pH (pH-100, pH-200, pH-500) microsensors (https://unisense.com/product-category/sensors-electrodes/) inserted into the sediment through 1-cm spaced pre-drilled holes in the core liner. Oxygen, pH, and redox microsensors were calibrated approximately 0.5 hours prior to each core measurement using Unisense calibration kits (https://unisense.com/products/calibration-kits/). Chilled top water from the box core was replaced at the surface of the subcore for microsensor measurements requiring an external reference electrode (RD-100, RD-200, pH-100, pH-200). For these measurements, the reference electrode was submerged in the top water for downcore measurements of pH and redox potential.

Oxygen microprofiles were measured in 35 subcores; these data are available in a data release, Shapiro and others, 2026. Figure 10 indciates the concentration of oxygen measured in the surface (1 cm) of each core; Figure 11 plots the full depth profiles. pH microprofiles were measured in three subcores and redox microprofiles were measured in 4 subcores before the last remaining pH and redox microsensors broke. Porewater was extracted using Rhizon (Rhizosphere Research Products, Wageningen, Netherlands) samplers and measured for pH using an Oakton pH 6+ hand-held meter (Environmental Express, Mount Pleasant, South Carolina) when pH microsensors were no longer available. The Oakton pH meter was calibrated with three pH buffer solutions, 0.5-2 hours before each subcore measurement.

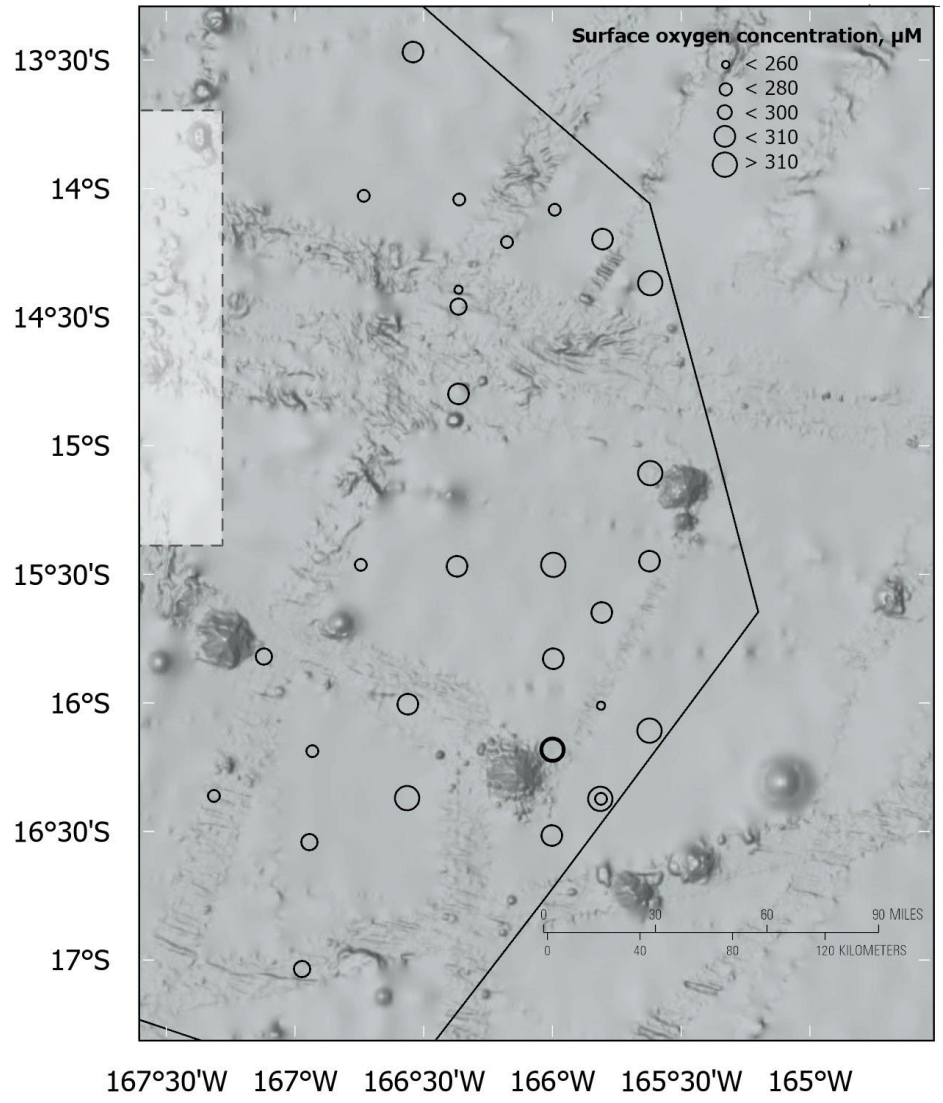

Figure 10. Map of oxygen concentrations in the top 1cm of sediment cores. These data and entire core length oxygen concentration data are included in Shapiro and others, (2026). Map data sources: ESRI, TomTom, Garmin, FAO, NOAA, USGS © OpenStreetMap contributors, and the GIS User Community, General Bathymetric Chart of the Oceans (GEBCO); NOAA National Centers for Environmental Information (NCEI)

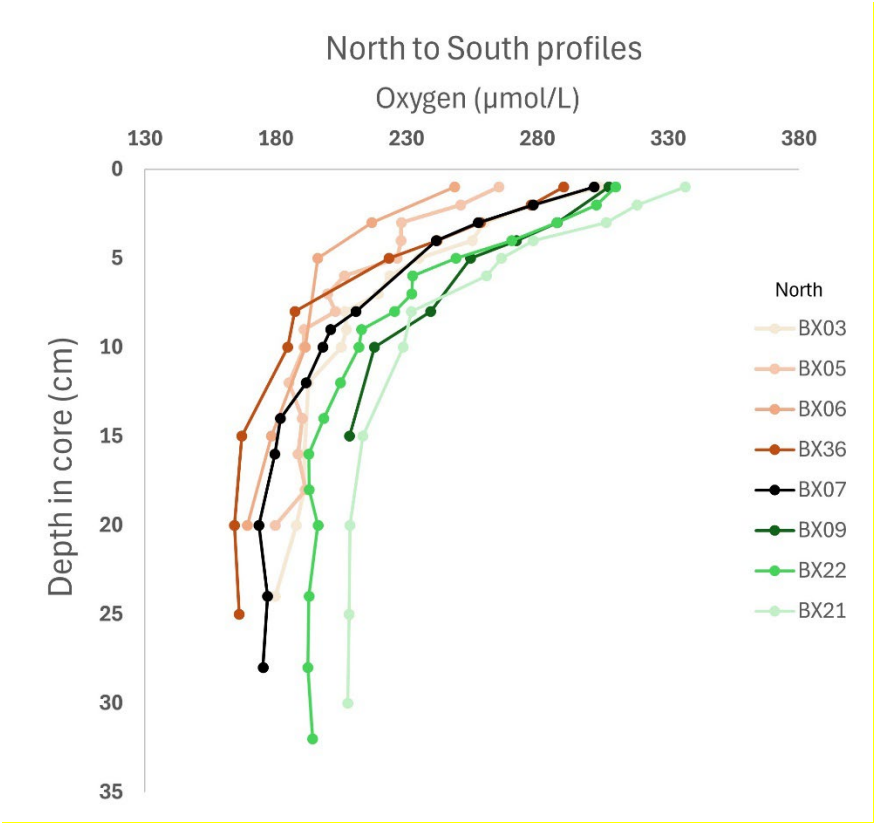

Figure 11. Profiles from several boxcores showing north to south range of oxygen concentrations. These data, and entire core length oxygen concentration data are included in Shapiro and others, (2026).

Porewater was extracted from one subcore (PC02) from each box core (n = 35) using Rhizon samplers at 2-cm intervals from 0-10 cm, 4-cm intervals from 10-30 cm, and 8 cm intervals from >30 cm. A total of 377 samples were collected for nutrient analysis and 377 samples were collected for trace metal analysis. Procedural duplicates were collected for nutrients and trace metal analysis from at least two intervals in each core.

Mercury subsampling

Porewater and sediment were sampled from one subcore (PC04) from each box core (n = 35) for total mercury and methylmercury analysis. Full length cores (n = 20) were sampled at 2-cm intervals from 0-10 cm, and 4-cm intervals from 10-30 cm. Short cores (10 cm, n = 15) were sampled at 5-cm intervals.

Nodule samples intended for mercury (Hg) measurements were collected from 13 box cores (Table 5). When possible, Hg push core samples were taken from same location in box core. Hg analyses are to be carried out at the University of California Santa Cruz in collaboration with the USGS Global Seabed Minerals and Resources Project.

Table 5. Stations where full and short subcores were sampled for mercury (*indicates that PC01 was also sampled for downcore genomics at the same intervals as PC04)

Core #	Near node	PC04
BX03*	7L	Full core
BX04	8K	Full core
BX05	8J	Upper 10 cm
BX06	8I	Upper 10 cm
BX07*	8H	Full core
BX08	8G	Upper 10 cm
BX09	8F	Full core
BX10	6F	Upper 10 cm
BX11	4E	Full core
BX12*	5DE	Full core
BX13	3C	Upper 10 cm
BX14	5CD	Full core
BX15	5B	Full core
BX16	7C	NA
BX17	10A	Upper 10 cm
BX18	11A	Full core
BX19	11A	Full core
BX20	10B	Upper 10 cm
BX21*	7D	Full core
BX22	7E	Upper 10 cm
BX23	10C	Full core
BX24	10B	Upper 10 cm
BX25	11B	Full core
BX26	12A	Upper 10 cm
BX27	12B	Full core
BX28	11C	Upper 10 cm
BX29	10D	Full core
BX30	12C	Upper 10 cm
BX31	12D	Full core
BX32	12F	Upper 10 cm
BX33	11G	Full core
BX34	10H	Upper 10 cm
BX35	9H	Full core

BX36	8Isouth	Upper 10 cm
BX37*	6J	Full core
BX38	16A	Full core

Sediment mineralogy and geochemistry

The sediment mineralogy and geochemistry subcore (PC06) was secured with flower foam, stored upright in a refrigerated room, and cold-shipped to the USGS Core Laboratory in Santa Cruz, CA for further analysis. This core will be CT and gamma scanned for relative and absolute density, then split and imaged. Half of each split core will be preserved as an archive sample, and half will be subsampled for sediment mineralogy and additional geochemical analyses, including major, minor and trace elements.

Radon flux from sediment

The flux of radon from sediment (0-4 cm) was measured shipboard in 10 box cores using a Durridge Company Inc. (Billerica, Massachusetts) Bulk Emission Chamber and Rad-7 radon Detector (Table 6). One-to-two 4-cm plastic fences filled with surface sediment and porewater were subsampled from the box core and stored in a cold laboratory van until analysis. The same sediment samples will also be measured for radium-226 at PCSMC to compare measured and estimated fluxes of radon from seafloor sediments analyzed for radium-226 at PCMSC.

Radon flux from ferromanganese mineral samples (surface and buried nodules, or coated volcanics for BX13) were collected from 8 box cores. Radon flux was measured shipboard using a Durridge Bulk Emission Chamber and Rad-7 detector and measurements will be continued at the USGS Global Seabed Minerals and Resources Project in Santa Cruz, CA.

Table 6. Stations where measurements for radon flux from nodules and/or sediment were collected.

Core #	Near node	Rn flux in sediment	Rn flux in ferromanganese minerals
BX03	7L	x	x
BX04	8K	x	
BX05	8J		x
BX07	8H	x	

BX08	8G	x	
BX13	3C	x	
BX16	7C		x
BX18	11A	x	x
BX21	7D	x	
BX24	10B	x	x
BX28	11C	x	x
BX31	12D	x	x
BX33	11G	x	x

Organic Geochemistry summary

Sediment samples were collected from 30 discrete box cores spanning a range in manganese nodule distribution, abundance, and morphologies. A designated push core (PC03) sampled the upper 30 cm of each box core, which was subsampled at 2-cm intervals, yielding 363 individual samples for characterization of sedimentary organic carbon (OC). Samples were collected in pre-combusted glass jars and stored frozen. Bulk sedimentary OC elemental and isotopic analyses will be made throughout push cores for OC quantification and initial characterization. This will include % total organic carbon (TOC), % total nitrogen (TN), C/N ratios, $\delta^{13}C$, and $\delta^{15}N$ via elemental analyzer isotope ratio mass spectrometry, (EA-IRMS). A subset of samples will be analyzed for OC compound classes (i.e., lipids, acid-soluble material, and acid-insoluble material) to evaluate OC bioavailability and provenance. Additional compound specific measurements (i.e., lipid biomarkers, amino acid isotopes) may provide further bioavailability and provenance information.

Rock samples were also collected on 2026-604-FA for carbon analysis. Sample material mainly included nodules and occasionally volcanic rock material. For box cores that had distinct nodule morphologies and/or abundant sample material, several nodule pieces were selected. A total of 26 rocks were collected from 26 discrete box cores, rinsed with filtered seawater to remove surface sediment, and stored frozen. On land, rocks will be crushed and analyzed for bulk OC elemental and isotopic analyses (TOC, TN, C/N ratios, $\delta^{13}C$ values, and $\delta^{15}N$ values) via EA-IRMS. If enough carbon is present in the rocks, additional compound class or compound specific measurements may be made to compare sedimentary carbon with carbon in the rocks.

References

Boström, K., 1973. The origin and fate of ferromanganoan active ridge sediments: Stockholm Contributions in Geology, v. 27.

Gurvich, E. G., 2006. Metalliferous sediments of the world ocean: fundamental theory of deep-sea hydrothermal sedimentation (p. 416). Berlin: Springer.

Lisitzin AP, Bogdanov YuA, Mudmaa IO, Serova VV, Zverinskaya IB, Lebedev AI, Lukashin VN, Gordeev VV, 1976. Metalliferous sediments and their genesis. In: Lisitzin AP (ed) Geological and geophysical research in the Southeast Pacific. Nauka, Moscow, pp 289-379.

Mizell, K., Hein, J.R., Au, M., and Gartman, A., 2022. Estimates of metals contained in abyssal manganese nodules and ferromanganese crusts in the global ocean based on regional variations and genetic types of nodules, in Sharma, R., ed., Perspectives on deep-sea mining: Cham, Switzerland, Springer, p. 53–80, https://doi.org/10.1007/978-3-030-87982- 2_3.

NOAA., 2026. Mapping the Seafloor for Critical Mineral Resources. National Ocean Service website, https://oceanservice.noaa.gov/deep-seabed-mineral-resources/mapping.html

Shari J. Preece, John A. Westgate, Becky A. Stemper, Troy L. Péwé; Tephrochronology of late Cenozoic loess at Fairbanks, central Alaska. GSA Bulletin 1999; 111 (1): 71–90. doi: https://doi.org/10.1130/0016-7606(1999)111

Strakhov N., 1976. Problems of geochemistry of recent ocean lithogenesis. Nauka, Moscow

Tay, S., Browne, R., & Berrtoli, O., 2023. Cook Islands polymetallic nodule deposit–Technical report and supporting documentation for The Cook Islands polymetallic nodules resource estimate (Resource estimation and-classification)(p. 219). Cook Island.

Paired data releases

Addison, J. A., Caissie, B. E., and Gartman, A. 2026. Surface sediment portable XRF geochemistry of the American Samoa EEZ abyssal plain collected during cruise 2026-604-FA (ver. 1.0, May 2026): U.S. Geological Survey data release, https://doi.org/10.5066/P13PAHV2.

Adamczyk, K.B., Gartman, A., Favela, J., Mizell, K., Shapiro, I.M., Phan, K. 2026. Abundance and geochemistry of ferromanganese nodules and ferromanganese coated rocks from the Samoa Basin (2026-604-FA): U.S. Geological Survey data release, https://doi.org/10.5066/P149BW9Z.

This information product has been peer reviewed and approved for publication as a preprint by the U.S. Geological Survey.

Shapiro, I. M., Adamczyk, K. Gartman, A. 2026.Oxygen Data from sediment cores from the Samoa Basin: U.S. Geological Survey data release, 10.5066/P14JMPDV